**Supplemental Information**

# CD34$^+$KLF4$^+$ Stromal Stem Cells Contribute

# to Endometrial Regeneration and Repair

**Mingzhu Yin, Huanjiao Jenny Zhou, Caixia Lin, Lingli Long, Xiaolei Yang, Haifeng Zhang, Hugh Taylor, and Wang Min**
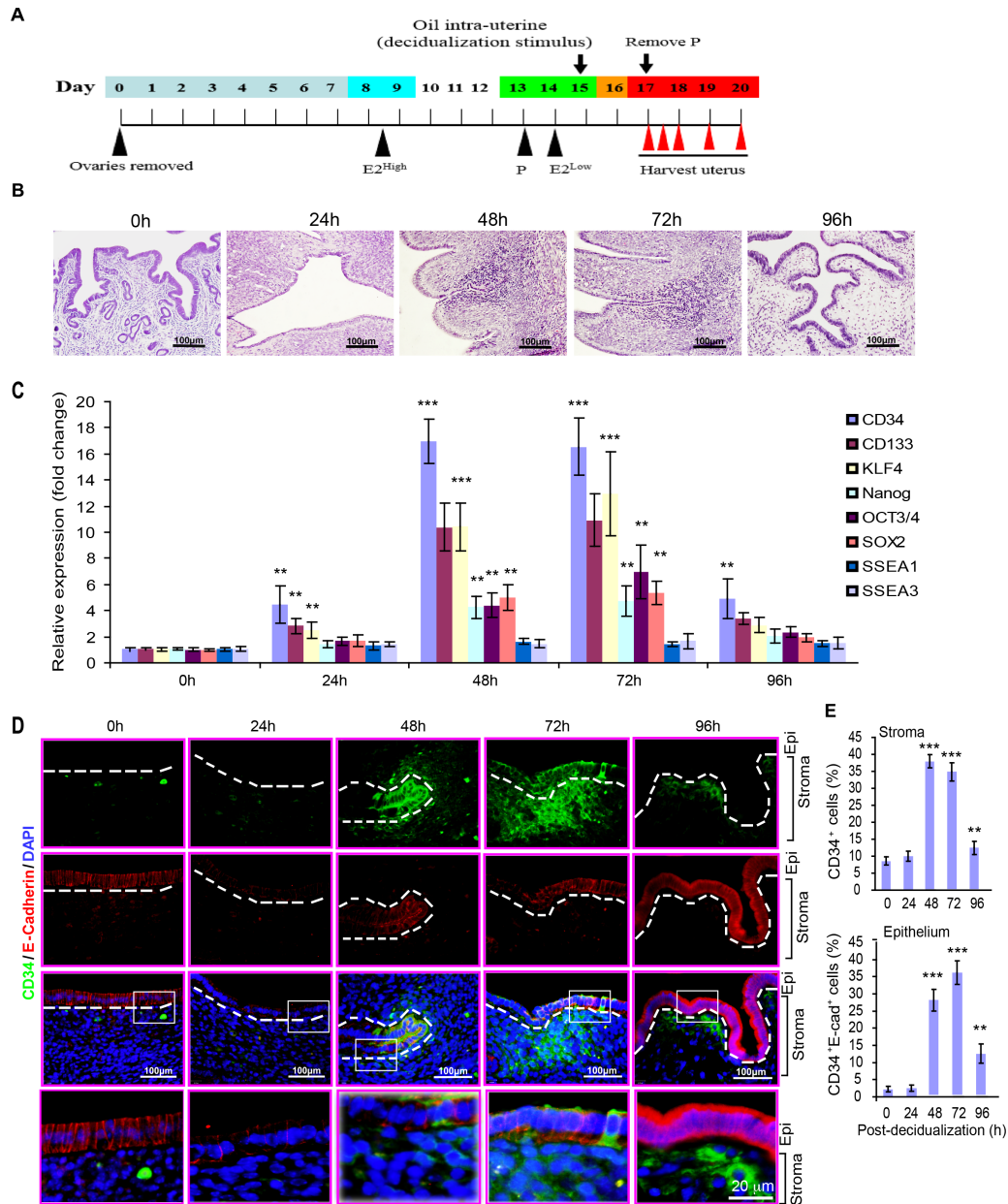
**Figure S1. Stem cell markers expression increased in the process of endometrial self-repair**. Related to Fig.1.

**A.** Establishment of mouse endometrial decidualization model. Ovariectomized mice were treated with estradiol (E2) injections and progesterone releasing implants to stimulate endometrial proliferation and differentiation. Decidualization was induced by injection of oil into one uterine cavity. Endometrial bleeding in response to removal of the progesterone implant was monitored by vaginal smears or blood collection with cotton pads. Uteri collected at 0, 24, 48, 72, and 96 hours post-progesterone (P4) withdrawal were used for histology and analysis of gene expression. **B**. Representative images of H&E staining for tissue sections from the mouse uterus. **C.** Mesenchymal stem cell markers were determined by qRT-PCR in mouse uterus. **D.** Immunofluorescent staining of CD34 and E-cadherin in tissue sections. An insert image with high magnification is shown underneath. **E.** Quantifications of CD34$^+$ cells in stroma, and of CD34$^+$E-cadherin$^+$ cells in the epithelium. All data are presented as means ± SEM, n=5, **, $P<0.01$; ***, $P<0.001$ (two-sided student's t-test). Scale bar: 100 μm (B,D).
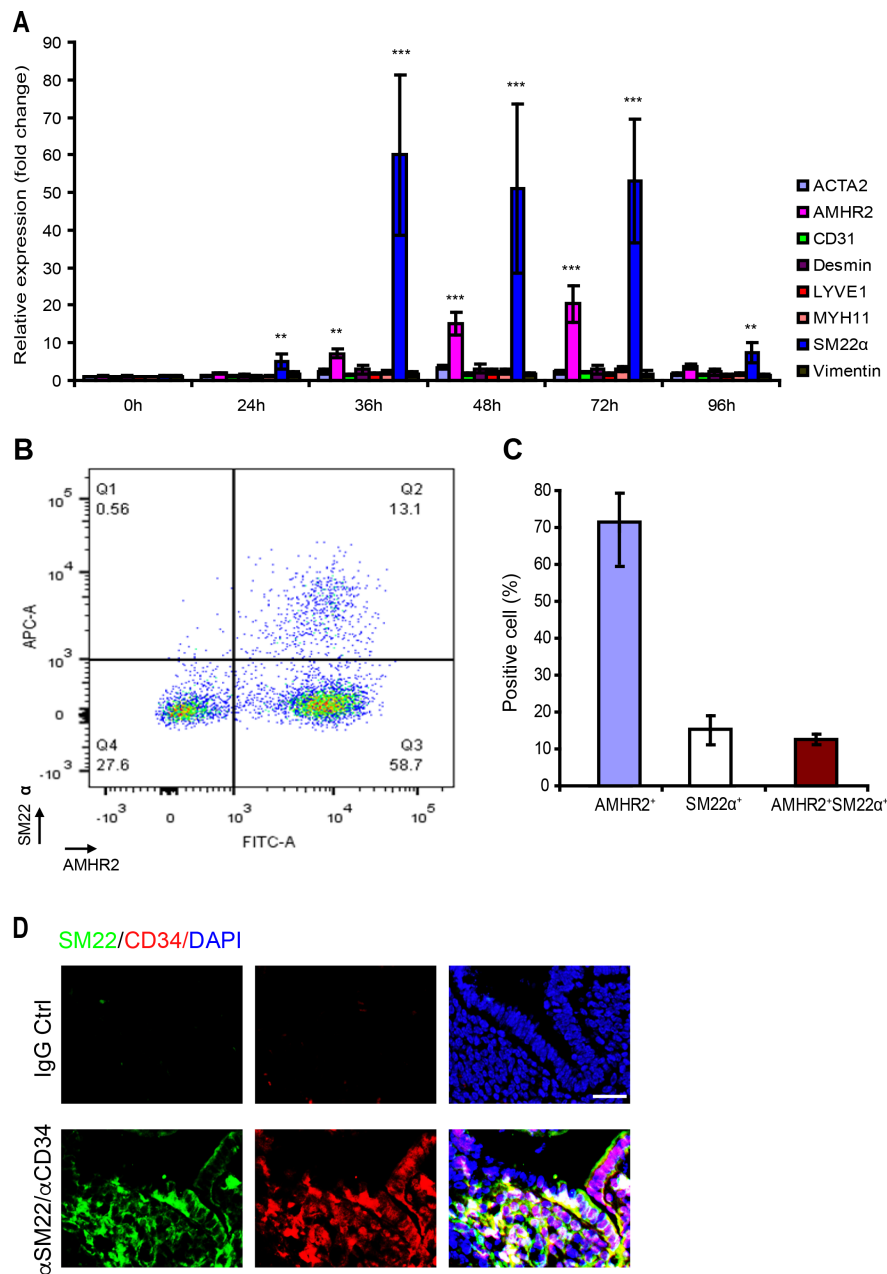
**Figure S2. SM22α positive cells are increased during the repairing process of the mouse uterus post-injury**. Related to Fig.1.

**A**. Uterine stromal markers were determined by qRT-PCR in mouse uterus at 0, 24, 36, 48, 72, and 96 hours post-injection of castor oil. All data are presented as means ± SEM, n=5, **, P<0.01; ***, P<0.001 (two-sided student's t-test). **B-C**. FACS analyses of AMHR2^{+}SM22α^{+} stromal cells in uterine from 2-month old mice. A representative FACS is shown in B. % of AMHR2^{+} and SM22α^{+} stromal cells were quantified (C). **D**. Isotype controls for immunofluorescent staining of SM22α and CD34 in tissue sections of Fig.2A (72 h time point samples were used). An isotype control for anti-CD34 antibody (abcam rabbit) and anti-SM22α (abcam goat) were used as primary antibodies followed by secondary antibodies (donkey anti-rabbit and donkey anti-goat). 25 μm (D).
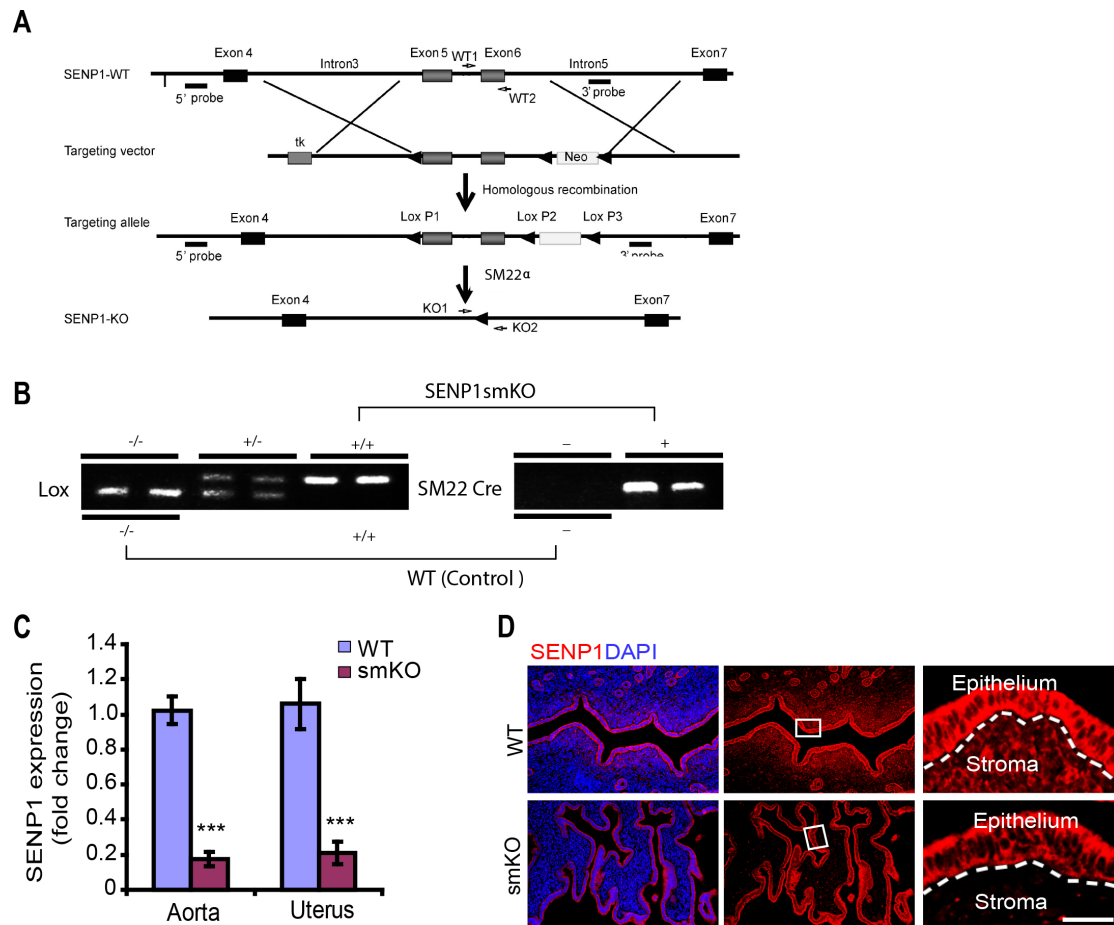
**Figure S3.** **Specific deletion of SENP1 in smooth muscle of SENP1-deficient mice**. Related to Fig.2.
**A.** SENP1$^{lox/lox}$ mice were generated based on homologous recombination. SENP1$^{lox/lox}$ mice were mated with SM22α Cre to obtain smooth muscle-specific SENP1-deficient (SENP1$^{lox/lox}$-SM22 Cre) mice.
**B.** Generation of SENP1$^{lox/lox}$ (WT) and SENP1$^{lox/lox}$-SM22Cre (SENP1smKO) mice. Tail genomic DNA was used to determine SENP1 deletion by PCR with KO primers adjacent to 5' of lox P1 (KO1) and lox P3 (KO2) to obtain heterozygous mice with a deletion of both the targeting region (the exons 5/6) and the Neo gene (SENP1$^{+/-}$). SENP1 KO mice were obtained by intercrossing between the heterozygous (SENP1$^{+/-}$) male and female. Representative genotypes are shown.
**C.** SENP1 was determined by qRT-PCR in uterus of WT and SENP1smKO mice at P21.
**D.** SENP1 deletion in the stroma, but not the epithelium layer of uterus. SENP1 was stained with anti-SENP1 antibody followed by DAPI counterstaining in uterus of WT and SENP1smKO mice at P21. 100 μm (D).
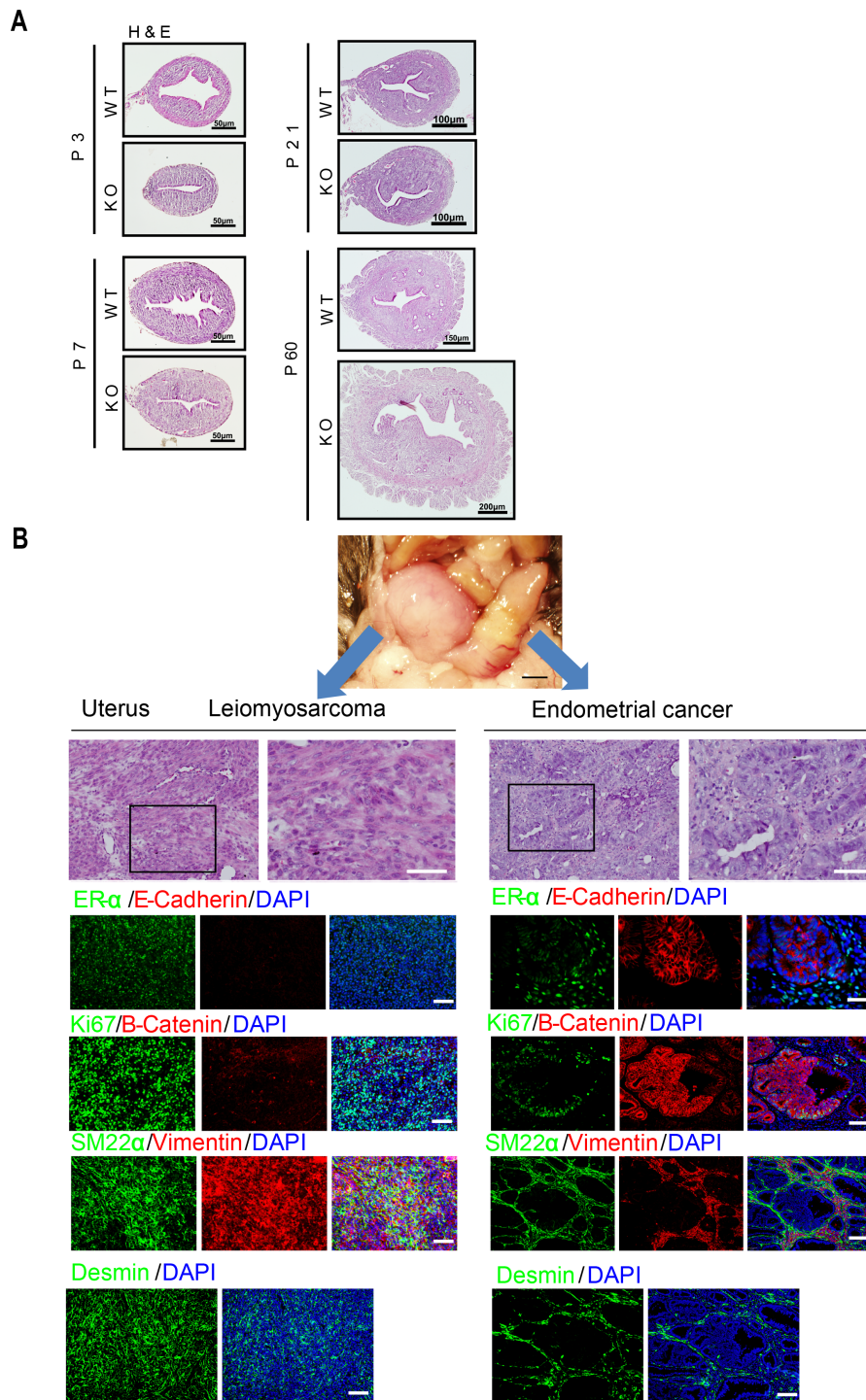
**Figure S4**. **Deletion of SENP1 in stromal cells significantly induces hyperplasia and tumor formation in aged mice.** Related to Fig.3.

**A**. Deletion of SENP1 in stromal cells significantly induces hyperplasia. Representative images and H&E staining of isolated uterus from WT and SENP1smKO mice at various ages (postnatal 3, 7, 21 and 50 days. Scale bar: 200 μm. **B.** Deletion of SENP1 in stromal significantly induces tumor formation in aged mice. H&E and immunostaining of uterine tumor sections from SENP1smKO mice at age of 12 months. Sarcoma/endometrial cancer are validated by several markers, including E-cadherin, β-catenin, Vimentin and desmin. Scale bar: 1.0 mm (whole tissue in B); 200 μm (immunostaining in B).
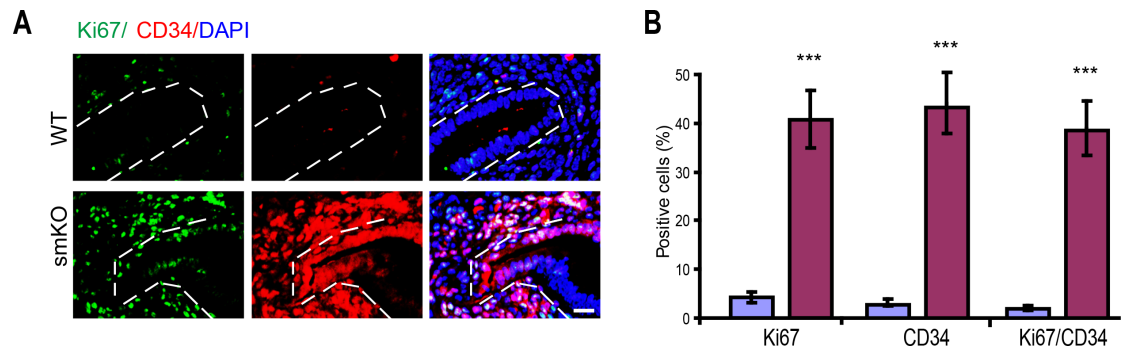
**Figure S5. CD34+ cells are proliferative.** Related to Fig.3.

**A.** Immunofluorescent staining of CD34 with proliferation marker Ki67 in uteri of WT and SENP1smKO mice at age of 9 and 9 months. **B**. Ki67+ and CD34+ cells are quantified. All data are presented as means ± SEM, n=5, **, *P*<0.01 ***, *P*<0.001 (two-sided student's *t*-test). Scale bar: 20 μm.
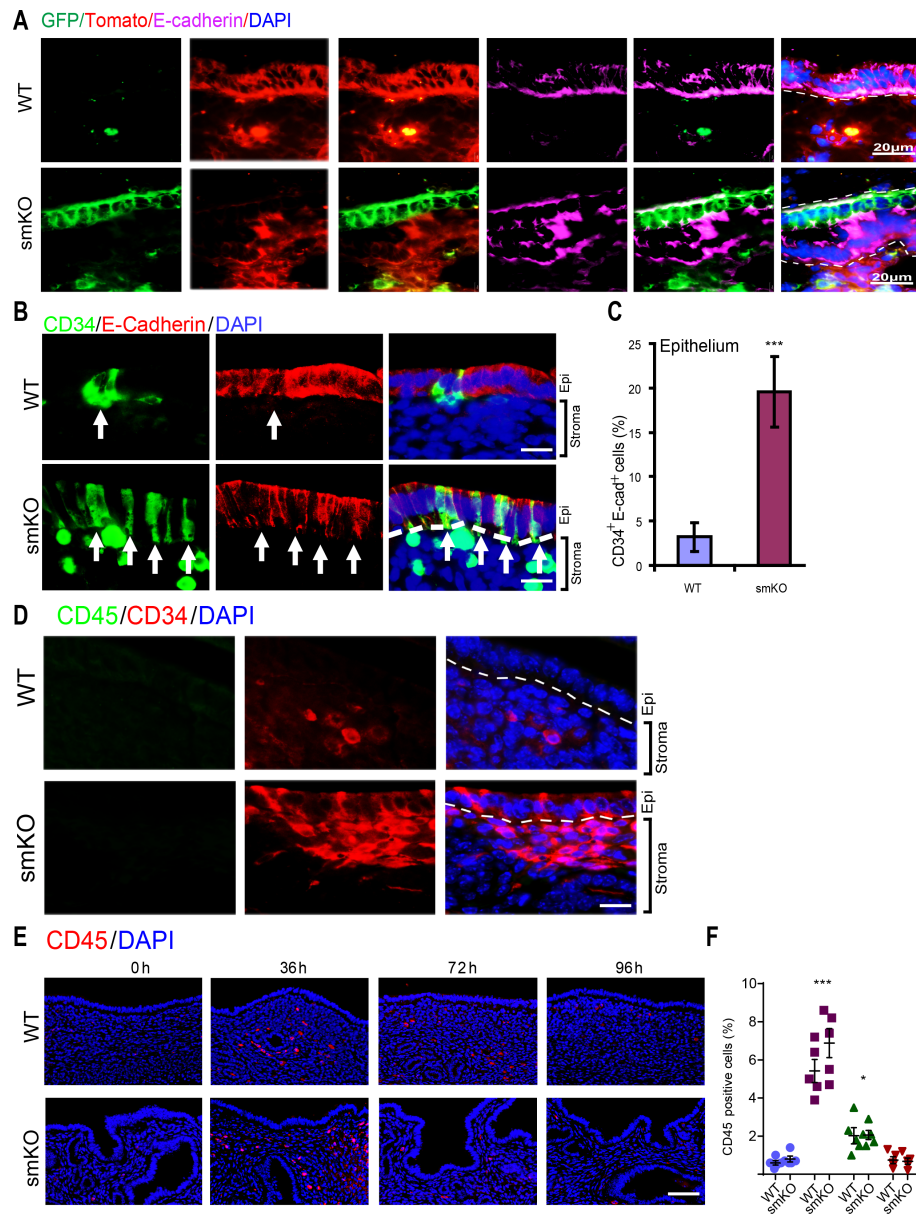
**Figure S6. SM22α⁺CD34⁺ stromal progenitor cells directly contribute to uterine hyperplasia.** Related to Fig.4.

**A.** Immunofluorescent staining with APC-conjugated anti-E-cadherin shown in purple) in uterine sections from mT/mG reporter mice (WT) and SENP1smKO:mT/mG mice at age 2-months old. DAPI was used for counterstaining of cell nuclei. Tomato (mT) indicates SM22α-negative cells whereas GFP⁺ as indicative SM22α-positive cells in stroma and epithelium layer. **B-C.** Co-immunofluorescent staining and quantification of CD34 and epithelial marker E-cadherin in uterine sections of 2-months old WT and SENP1smKO mice. White dash lines show the boundaries between endometrial stroma and epithelium. White arrows show CD34⁺ E-Cadherin⁻ cells in epithelial layer. **D.** Co-immunofluorescent staining of CD34 and leukocyte marker CD45 in uterine sections of 2-months old WT and SENP1smKO mice (n=5). **E-F**. Representative images and quantification of leukocyte marker CD45 in the uteri from a mouse endometrial decidualization model at 0h, 36h, 72 and 96 h post-P4 withdrawal (n=10). All data are presented as means ± SEM, *, P<0.05 ***, P<0.001 (two-sided student's t-test). Scale bar: 20 μm (A,B,D); 100 μm (E).
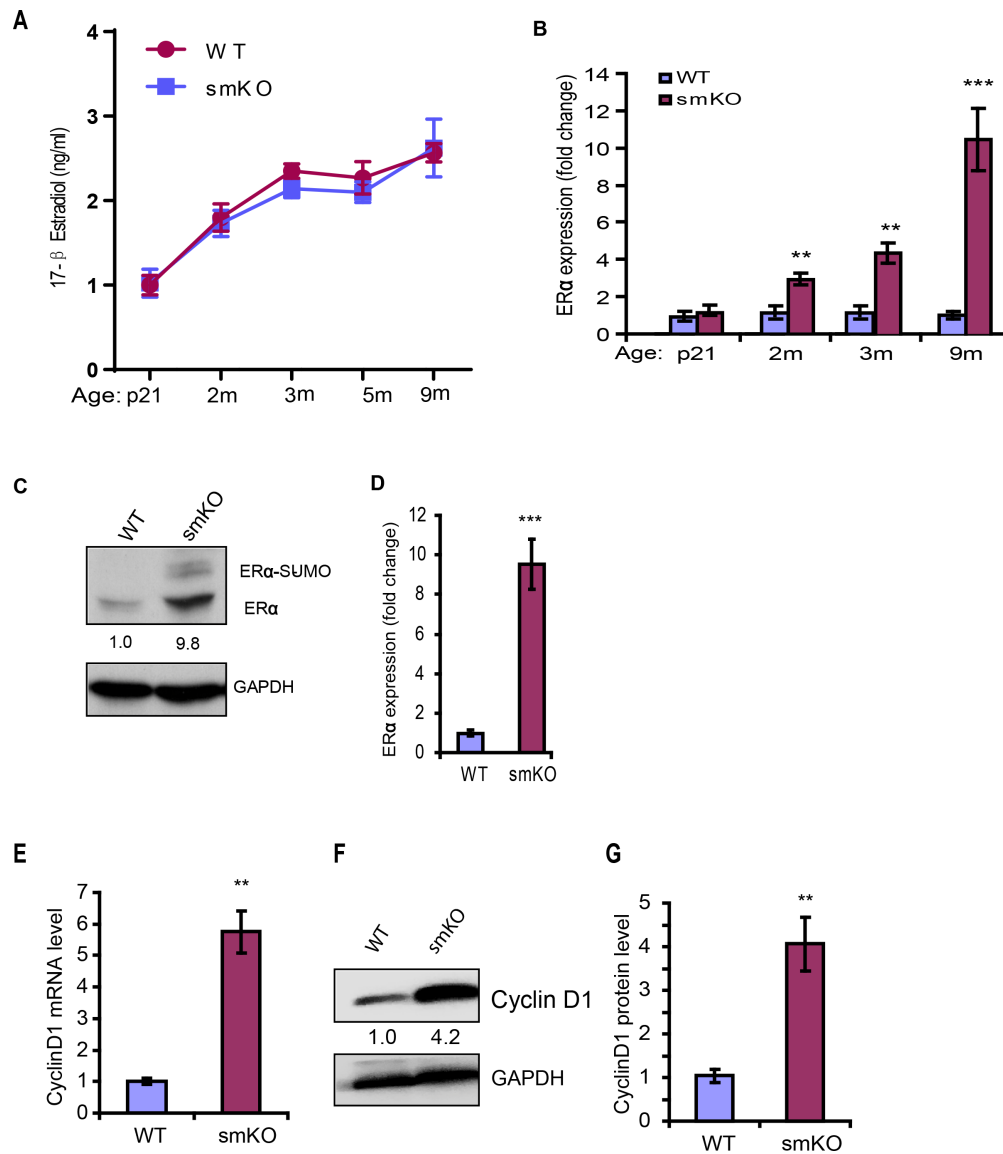
**Figure S7**. **Expression of ERα and Cyclin D1 significantly increased in SENP1smKO mice**. Related to Fig.6.

**A.** 17-β estradiol levels were not different in plasma between WT and SENP1smKO mice. Enzyme-linked immunosorbent assay (ELISA) analysis of 17-β estradiol in serum from WT and smKO mice at various ages.

**B.** ERα mRNA expression was determined by qRT-PCR in uterus from WT and SENP1smKO mice at various ages.

**C-D.** Immunohistochemical staining and quantification of ERα in uterine stroma and epithelium from 4-month WT and SENP1smKO mice.

**E.** Cyclin D1 mRNA expression was determined by qRT-PCR in uterus from 4-month WT and SENP1smKO mice.

**F-G.** Cyclin D1 protein expression and quantification in uterine from 4-month WT and SENP1smKO mice by Western blotting. GAPDH was used as a loading control.

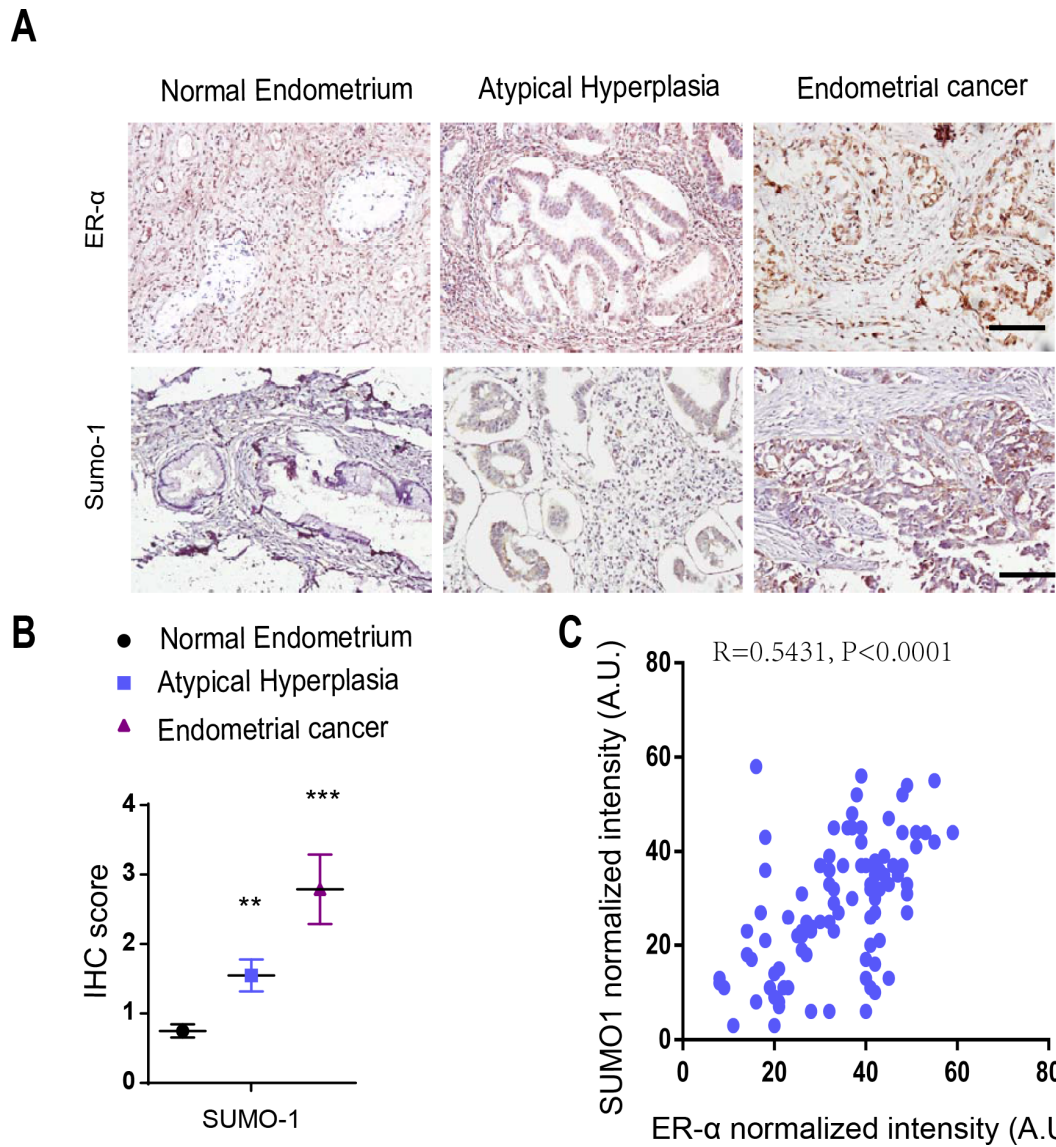All data are presented as means ± SEM, n=5, **, P<0.01 ***, P<0.001 (two-sided student's t-test).

**Figure S8**. **Expression of ERα and SUMO1 significantly increased in human endometrial cancer**. Related to Fig.7.

**A.** Immunohistochemical staining of ERα and SUMO1 in human endometrial cancer samples. Scale bar: 100 μm.

**B-C**. Relative mean intensity calculated using Image J for cell clusters from 97 endometrial cancer patients. Statistical significance at (R=0.5431, p<0.0001). (two-sided student's t-test).
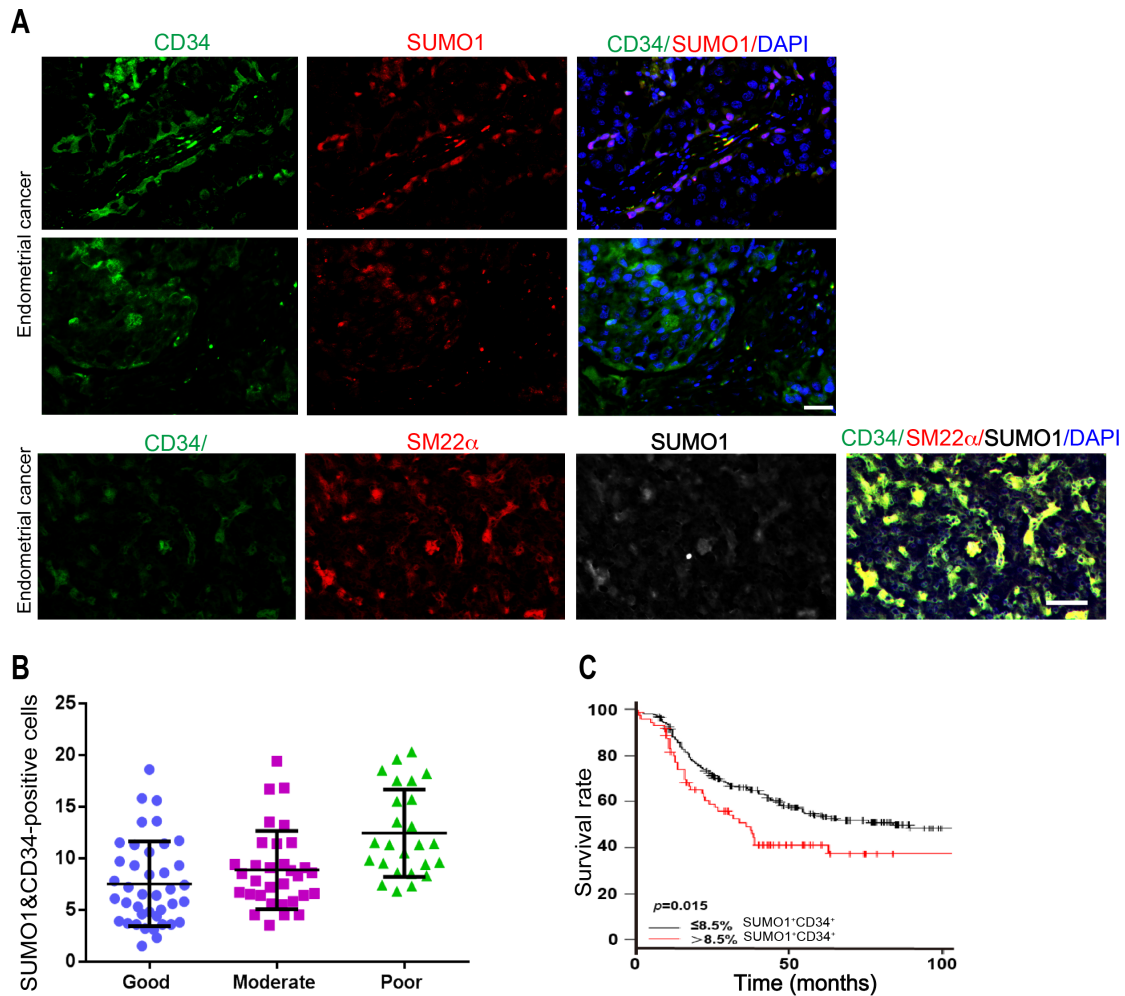
**Figure S9**. **Expression of CD34 and SUMO1 significantly increased in human endometrial cancer**. Related to Fig.7.

**A.** Immunofluorescent staining of CD34, SM22αand SUMO1 in human endometrial cancer samples. Scale bar: 50 μm. **B.** Statistical analysis of CD34$^+$ SUMO1$^+$ cells in human endometrial cancer with different histological differentiation (2-sided Student's t test). **C.** Kaplan-Meier curves for OS in human endometrial cancer with low (≤8.5%) or high ( > 8.5%) percentage of CD34$^+$ SUMO1$^+$ cells in human endometrial cancer (analyzed with log-rank test)